Total Energy Electronic Structure Calculations: From Silicon to Carbsn 60*

Atsushi Oshiyama

Fundamental Research Laboratories, NEC Corporation
Miyukigaoka, Tsukuba 305, Japan

Received July 12, 1093

We report microscopic total-energy electronic-structure calculations for the materiais ranging from typical semiconductors to exotic new inaterials. The calculations have been perforined within the local density approximation (LDA) in density functional theory. The results and their comparison with experiments elucidate success and limitation of LDA.

I. Introduction

To explain and then predict phenomena in nature on the basis of ab initio calculations are fascinating challenges in science. Local density approximation (LDA) in density functional theory[1] lias been shown to ɔe an effective tool for such challenges[2]: Although the LDA fails to describe excited states in condensed matters quantitatively[3], it provides very accurate structural and electronic informations about tlieir ground states. In this talk, I will present total-energy electronic-structure calculations within tlie LDA for several materials. I start with an issue of the Si vacancy which is a paradigm of defects il1 semiconductors, and also contains important aspects in semiconductor physics. I next report the results for microscopic mechanisms for arsenic substitutional adsorption on tlie Si(100) surface which is gencrally regarded as an initial stage of epitaxial growth. Finally, I discuss electronic striictures of dopeci fullerides. An emphasis is put on alkaline-ear :h doped fullerides which have recently been discovered to bc superconducting.

II. Calcule tion

Since details have been given elsewhere[4,5], I will give only a brief description of tlie calculational method. First, nuclei and core electrons are simulated by pseudopotentials which are generated by atomic (ionic) LDA calculations. They are normconserving[6] and have liigh transferability. Second, interactions among valence electrons are treated hy the LDA in density functional theory. For tlie exchange-correlation energy, we use tlie Ceperley- Alder form[7] as is parametrized by Perdew and Zunger[8]. Third, plane waves are used as basis to expand valence-electron wavefunctions and thus valence-electron charge density[9]. In large-scale calculations, electron-degrees-of-freedom is conveniently optimized to minimize the total energy, or in other words a.n effective Schrodinger (Kohn-Sham) equation is solved, by iterative methods. The preconditioned conjugate-gradient-method which we use is an example. We also use the conjugate-gradient-method to optimize nuclear(ionic)-degrees-of- freedom (geometry optimization). We adopt an alternative minimization procedure in whicli the electron-degrees-of-freedom and the ioriic-degrees-of-freeclom are optimized consecutively[10], in contrast with the simultaneous optimization[11]. The calculational conditions, such as the validity of the Kleinman-Bylander approximation[12], tlie sizes of supercells used in calculations, tlie cutoff energies in the plane-wave-basis sets, the number of li points in Brillouin zone for the integration, ctc, are well examined to obtain reliable results[4].

Tliis LDA describes severa1 aspects in condensed

*Invited ta k.

i.e., covalency, flexibility of bond network, i.e., elasticity, and effect of charge transfer among different atoms, i.e., ionicity, are satisfactorily described in the LUA. Electron correlation is not completely treated in the LDA, but it is partially included in the scheme. Phenomena in condensed matters are regarded as a competition among these interactions. Hence it is not surprising that the LDA nicely describes phenomena in real materials.

III. Vacancy in silicon

An example which exhibits such a competition is the vacancy in Si crystal. If we remove a. Si atom from tlie crystal, we have a vacancy which induces deep levels in the gap between valence and conduction bands. Tlie deep levels consist mainly of four sp^3 dangling bonds generated by removing tlie Si atom. Actually, a state named a_1 with totally symmetric linear combination of the dangling bond orbitals appears just below the valence-band-top. Tlie remaining three states with the symmetry of t_2 appear in the center of the gap. In the case of the neutral vacancy, two electrons are accommodated in this triply degenerate level. We thus expect Jahn-Teller type, symmetry-lowering distortion around the vacancy. This is a competition between hybridization, or tlie rebonding energy, and the elasticity. Further, we have more than one electron in the deep level so that electron correlation is also expected to play a role.

In fact, for negatively-charged vacancy V−, there has been a controversy about the effect of electron correlation. From the Electron Paramagnetic Resonance (EPR) measurement[13], the Jahn-Teller distortion is considered to take place, and the symmetry lowers from T_d to C_{2v}. But semiempirical molecular orbital theory combined with the estimate of Jahn-Teller energy does not lead to the ground state of this symmetry[14]. Hence, it has been argued that the electron correlation is important and its explicit inclusion, a.s in the configuration interaction treatment, is necessary to explain the experiment.

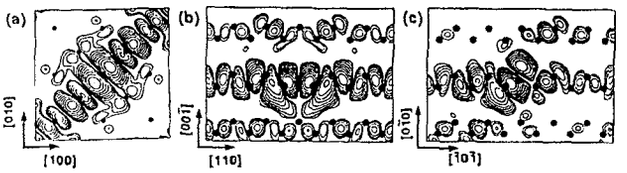

Figure 1: Contour plots of the wavefunction of the deep level in V^{-1}: (a) in the (001) plane, (b) in the (110) plane, and (c) in the (101) plane. The Si lattice sites are shown by solid circles, and the vacancy is situated at the center of each figure.

However, tlie LDA calculation provides nice results[5]. The total-energy optirnization for the 216-site supercell leads to a stable rebonded geometry in which both Jahn-Teller- type symmetry-lowering distortión and the breatliing-type symmetry-keeping distortion take place. The obtained geometry has the symnietry of C_{2v}, which is consistent with the EPR experiment. In the geometry each two of four dangling bonds forms a. pair, and there is an energy barrier from this geometry to another equivalent geometry in which different two dangling bonds form a pair. The calculated barrier is 0.12 eV which is comparable with the corresponding experimental value of 0.07 eV.

Figure 1 is a wavefunction of the deep level of V−. In general, wavefunctions of deep levels are considered to be localized. But a surprise in Figure 1 is, although it is indeed localized, the wavefunction is extendecl in an anisotropic fashion. There are atomic chains along {110} direction in diamond structure. The wavefunction of the cleep level of V^- extends along this direction. We also observe some distortions in the back-bond region around tlie vacancy. We can compare this wavefunction with Electron-Nuclear-Double-Resonance (ENDOR) measurement[15]. To quantify the comparison, we show both theoretical and experimental values of tlie wavefunction at each Si site around the vacancy in Figure 2. It is clear that the experimental values of the wavefunction along {110} direction is much larger than the values at another Si sites, in accord with the present calculation. The agreement between the calculation and the experiment is satisfactorily good.

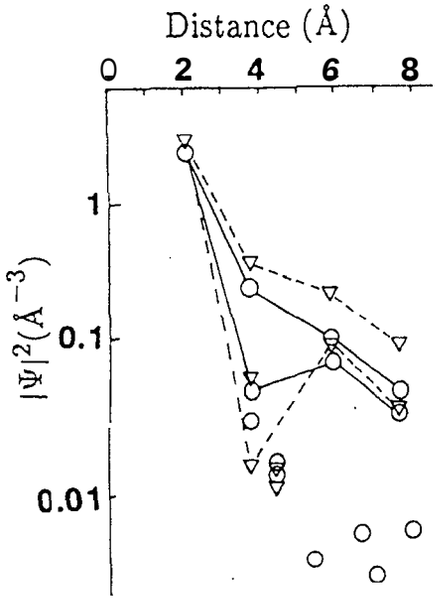

Figure 2: The amplitude of tlie wavefunction at nuclear sites plotted against the distance fiom the vacancy site. Calculated results are shown by circles and tlie ENDOR data are shown by triangles. The atomic sites on the zigzag chains in tlie {110} plane are coniiected by solid lines (calculated results) and cashed lines (ENDOR data).

IV. Substitutional arsenic adsorption on silicon (100)

The next example is tlie substitutional As adsorption on the Si(100) surface. This is regarded as an initial stage of heteroepitaxial growth of GaAs on Si which is of technological importance. The Si(100) surface exhibits a well-known dimerized structure: Each two of top-layer Si atoms forms a dimer and the dimers are lined up in one direction, leading to 2 × 1 structure. Atomic steps are always observed. The commonly observed are single-layer and bilayer steps. When the surface is slightly misoriented, e.g., inclined toward {110} direction by several degrees, it shows tlie bilayer steps dominantly; the bilayer step named DB in which the dimers on each terrace are parallel to tlie step edges.

In case that As is adsorbed on this Si(100) by one monolayer, what we would naturally expect is the 1 x 2 structure with As dimers: The As atoins are adsorbed on the 2 x 1 Si surface, break the existing Si dimers, and form new As dimers. The resulting As dimers are rotated by 90° compared with the original Si dimers just because of a inherent feature of the diamond structure. This is what is actually observed in experiments at low temperature ($T < 400°C$)[16,17]. At higher temperature ($400°C < T < 600°C$), however, It is observed[16,17] that the surface shows the 2 x 1 dimerized structure with the top-layer As dimers unrotated compared with the original Si dimers.

To explain this surprising phenomenon Alerhand et al. have performed total energy calculations for the two types of bilayer steps for the As-covered Si(100)[18]. They have found that one type where the As dimers are parallel to the step edges has lower energy than the other where the dimers are perpendicular to the edges. This implies that the dimer-rotated 1 × 2 structure made by tlie As adsorption is metastable. A counter-argument that substitutional As adsorption occurs on a terrace has come from Tromp et al. based on low-energy electron inicroscopy and scanning tunneling microscopy (STM) measurements[19]. They consider that tlie As atoms on top replace the underlying Si atoms, leading to a 2 x 1 reconstruction of the As-covered surface. In both arguments, the relaxation of the surface stress is the only driving force for the phenomenon: It is considered to be relaxed at the step edges in the forner, and on the terrace in the latter. Further, little is known about reaction pathways toward the lower energy states.

We here propose a microscopic mechanism to explain this phenomenon occasionally called the sublattice dilemma. We present the total-energy electronic-structure calculations which support a dimer exchange mechanism in which As dimers adsorbed on top of the dimerized Si surface substitute the sub-surface Si atoms, and then the Si atoms displaced diffuse to another site on the terrace or, more likely, to step edges. The driving force for the exchange is not surface-stress as was imagined but newly discovered π bonding bettveen the top-layer and the subsurface-layer Si atoms[20].

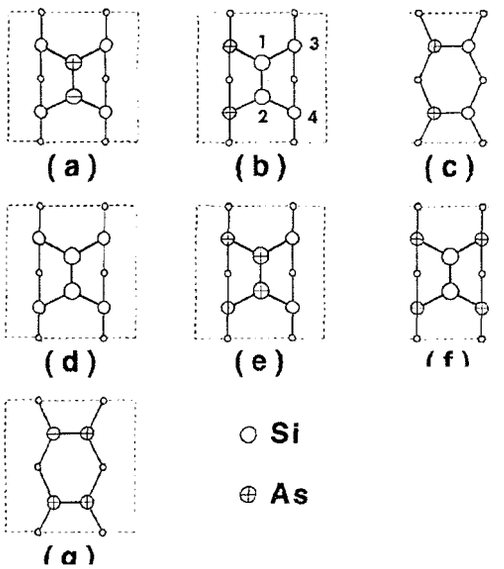

Figure 3: Schematic top vieívs of several geometries iii tlie exchange rneclianism for substitutional As adsorption on Si(100). Tlie open and the crossed circles represent Si antl As atoms, respectively. (a) As dimer on Si(100), (b) Si dimer on underlying As (tlie numbered Si atoms are referred in text), (c) As-Si heterodimer on Si(100), (d) Si dimer on Si(100), (e) As dimer on underlying As antl Si atoms. (f) Si dimer oii underlying foui As atoms, antl (g) As dimers oii Si(100). Each figure depicts a half of the 2×2 periodic c-tll iii lateral directions which is used in the present calculations.

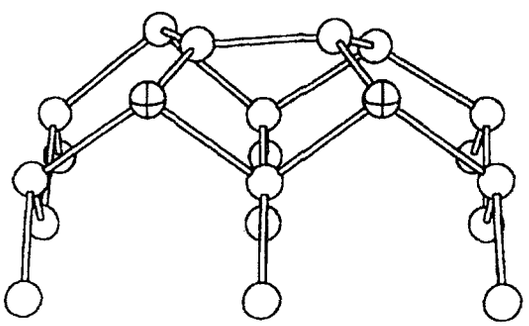

Figure 4: Stable geometry after substitutional As adsorption on Si(100), corresponding to the schematic illustration of Fig. 3 (b). The open and the crossed spheres denote tlie Si and As atoms, respectively.

The first geometry in the dimer exchange process is shown in Fig. 3(a): Arsenic atoms break a Si dimer and an As dimer is formed oii the Si 2 x 1 dimerized surface. The As dimer is rotated by 90° with respect to tlie Si dimers. We have examined a dimer exchange process in which tlie troo As atoms in Fig. 3(a) substitute the subsurface Si atoms. The resulting geometry is a Si dimer on tlie 2 As and 2 Si atoms (Fig. 3(b)). The calculated heat of formation of this reaction is calculated to be 0.7 eV: The dimer exchange is an exothermic reaction.

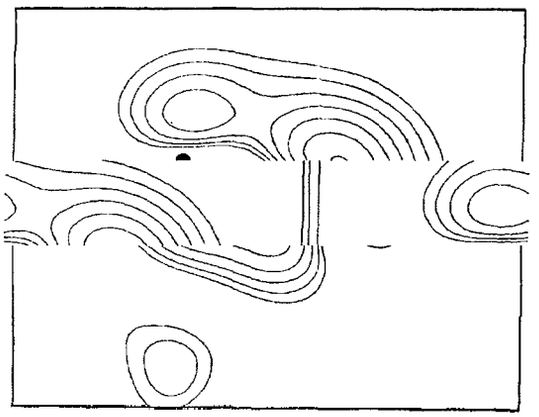

Figure 5: Charge density of an occnpied state near the surface Brillouin zone boundary ($k = \pi/2a_0(3/8, 3/8, 0)$). A π bond between Si(2) and Si(4) denoted by the solid circles is shown on the vertical plane cutting tlie two Si atoms. The value of tlie highest contour is 3.5×10^{-3} e/(a.u.)^3, and tlie subsequent contours differ by a factor of 1.65.

The geonietry after dimer exchange is accurately determined by the LDA calculation as in Fig. 4. We observe a flexible reconstruction of the top layer Si atoms. They are buckled aiicl flattened considerably. As a result, the distance between the top-layer Si and the sub-surface Si becomes shorter than the distance between the two top-layer Si atoms. The wavefunction below the Fermi-level in this geometry plotted in a plane which contains the top-layer Si and the sub-surface Si is shown in Fig. 5. Tlic wavefunction exhibits π-bonded character between the top-layer aiid the sub-surface Si atoms. In other words, electronic structure changes from metallic to semiconducting upon tlie dimer exchange. This is tlic origin of the energy gain in the exchange process.

Next, these Si atoiiis are desorbed from the site (Fig.3(b)) and diffuse to another site on a terrace (Fig.3(d)), or a step edges. Tlie remaining atoms form two As-Si hetero-dimers as in Fig.3(c). The total-energy difference between the iiiitial and the final states in this reaction is calculated to he 0.4 eV. Again this reaction of tlie desorption and the subsequent diffusion is exothermic. The next dimer exchange could take place oll tlie As-Si hetero-dimer site. New As atoms come to break the hetero-dimer and form a As dimer (Fig.3(e)). These As atoms again substitute the subsurface Si atoms (Fig.3(f)), and then tlie displaced Si

atoms coul:d diffuse away (Fig.3(d)). The calculated heat of for nation is 0.8 eV for this exchange reaction, and it is 0 6 eV for the subsequent diffusion reaction. Both are exothermic reactions.

Tlie As dimers formed by these consecutive exothermic reactions (Fig.3(g)) are unro- tated compared with tlie starting Si dimerized surface. Tlie sublattice-dilemma is naturally explained. Of course there are several com peting process, such as As diffusion process before tlie exchange. But what I like to emphasize is that the diiner exchange process is exothermic, and the reason for tlie exothermicity is tlie new π-bonded structure betweeii tlie top-layer and the sub-surface layer Si atoms, or in other words, the flexible reconstruction in tlie resulting geometry.

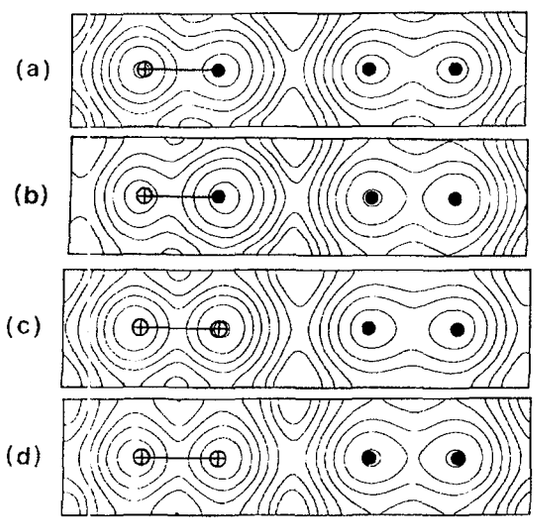

Figure 6: Calculated tunneling current density for the As-Si heterodimer witli bias voltage (a) V =–2 eV, (B) V = -1 eV, and the As dimer with (c) V =–2 eV, and (d) V = -1 eV. In tlie right half of each figure, the current densitg for tlie averaged Si asgmmetric dimer is shown. Tlie crossed circles denote the position of As atoins. Tlie values of the higliest contour are 3.10 x 10^{-4} e/(a.u)^3 in (a), **1.85** $\times 10^{-4}$ e/(a.u)^3 in (b), 3.88 x 10^{-4} e/(a.u)^3 in (c) and 1.70 x 10^{-4} e/(a.u)^3 in (d), respectively. Tlie subsequent contours differ by a factoi of 1.5.

Fig. 6 is the calculated images in scanning tunneling microscopy (STM) of the As- Si hetro-dimer and the As dimer, along with the image of the Si dimer. We note several interesting features. In the -4s-Si hetro-dimer, The As site becomes brighter with increasing tlie bias voltage (with incliicling lower states below the Fermi level). This is the consequence that the energy of tlie As dangling bond, which constitutes the As-Si hetero-diiner, is lower than that of the Si dangling bond. We observe a change in brightness with varying the bias voltage also for the As dimer. In any case, we find significant difference among the Si dimer, the As dimer and the As-Si hetero-dimer. Hence experimental observation of tliese iinages could be an evidence for the dimer exchange mechanism presented here.

V. Alkaline-earth doping in solid C_{60}

We now move to a story of C_{60} which has a unique sliape of a soccer ball with 60 carbon atoms located at tlie 60 vertices of tlie ball[21]. The carbon soccer balls were found to be condensed in a crystalline form[22], and it is a semiconductor with an energy gap of about 2 eV[23,24]. Alkali-atom doping makes this material metallic and superconducting with the transition temperatiire T_c more than 30 K[25]. Electronic structures of tlie pristine C_{60} and alliali-doped C_{60} are summarized as follows[26]. (i) In the pristine C_{60} which is of the face center cubic (fcc) structure, the highest occupied band (valence band) named h, is fivehold degenerate, and tlie lowest unoccupied band (conduction band) named t_{1u} is triply degenerate at the Brillouin zone center. (ii) Tlie next lowest conduction band named t_{1g}, also triply degenerate, is located about 1 eV above the t_{1u} hand. (iii) In alkali-doped C_{60} (fulleride) A_xC_{60}, electron of alkali atoms are transferred to π orbitals of C_{60} balls, since tlie ionization energy of an alkali atom (K, Rb, Cs) is much smaller than that of a C_{60} ball. (iv) In tlie superconducting fcc A_3C_{60}, the alkali atoms occupy every tetrahedral and octahedral interstitial sites, and the t_{1u} band is half filled with the transferred electrons. Hence this material is an ionic metal. (v) The A_6C_{60} is experimentally an insulator. this is simply explained by the fact that 6 electrons are enough to fill the t_{1u} conduction band. (vi) It is also found[27] that there is an unique linear relation between the observed T_c and the calculated Density of States near Fermi level

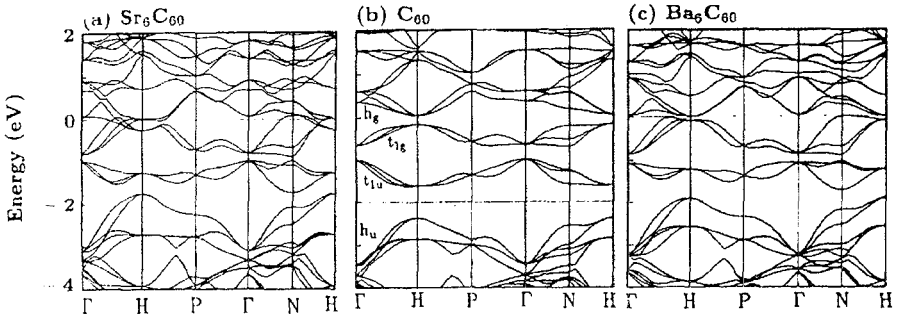

Figure 7: Energy-band structures of *(a)* Sr_6C_{60}, (b) hypothetical undoped bcc C_{60}, and (c) Ba_6C_{60}. Energy is measured from the Fermi level denoted by the horizontal lines.

in pressurized K_3C_{60} and Rb_3C_{60}.

It was iecently found that alkaline-earth doping also produces superconductivity: Ca_5C_{60} ($T_c = 8K$)[28], Ba_6C_{60} ($T_c = 7K$)[29], ancl Sr_6C_{60} ($T_c = 4K$)[30]. The latter two are particularly interesting since their crystal structure (body ceiiter cubic (bcc)) and the composition are identical to alkali-doped A_6C_{60} which is an insulator. Naive thinking leads to a conclusion that Ba6C60 ancl Sr_6C_{60} are also insulating, since full charge transfer results in the complete occupancy of the t_{1u} ancl the next lowest t_{1g} conduction bands. We have found that tliis is not tlie case, however. The reason is hybridization between π orbital of the ball ancl tlic alkaline-earth orbitals, in particular, d orbitals[31].

Fig. 7 shows calculated eiiergy bands of Sr_6C_{60} and Ba_6C_{60}. In Sr_6C_{60}, the t_{1u} conduction bands are completely occupied. 'Tlie ncxt lowest band t_{1g} is partially occupied, since it hybridizes with $4d$ state of Sr and tlie upper π band. As a result, Sr_6C_{60} is the first example of seniimetallic fullerides. A possible reason for tliis strong hybridization could be a reduction of the inter-ball distance: In Sr_6C_{60}, tlie distance between C_{60} clusters is 9.53 A, 5% shorter than the value in pristine C_{60}. But this is not the answer. Fig.7(b) is the energy bands of hypothetical undoped bcc C_{60} which lias the identical structure with Sr_6C_{60}. The energy bands of this hypothetical C_{60} are significantly different from those of Sr_6C_{60}. Rather, tlic bands in Fig. 7(b) is almost identical to the bands of K_6C_{60}[32].

Tlie situation is the following. For a neutral Sr atom, tlic 5s level is occupied by 2 electrons. Tlie ionization energy is smaller than that of C_{60} cluster so that the electron is transferred to π orbitals in Sr-doped C_{60}. When the Sr is ionized, however, tlie 4d level is lowered and close to tlie $5s$ level. Further, in Sr_6C_{60} the Sr atom has a. higli coordination nuniber; there exist 5 or 6 neighbor carbon atoms. This coordination number favors tlie d state with which the π orbitals are hybridized. Hence tlie clectron is transierred from the 5s state to tlie π state, and partially transferred back to tlie $4d$ state. This combination of charge transfer ancl the hybridization renders the material seinimetallic. At the same time, tlic interball distance is reduced; i.e., the hybridization works as a glue for tlie soccer balls.

In Ba_6C_{60}, the situation is cssentially same with Sr_6C_{60}. Fig. 7(c) is the energy bands of Ba_6C_{60}. It is again a semimetal. But in this case, the $5d$ level of Ba is slightly higher than the $4d$ level of Sr. Then the mixing between the t_{1g} and tlie $5d$ becomes less prominent so tliat the density of states near the Fermi level is smaller than that in Sr_6C_{60}. A ncw feature, however, has come up in this case. That is tlie inter-ball or the intra-ball state. This state has the amplitude both within and between the soccer balls, and not on atomic sites. Tlie intra- and inter-ball state is an analogy of the interlayer state in graphite intercalation coinpounds, and generally exists in anisotropic materials or the materials with large vacant spaces. In the case of Ba_6C_{60}, the state is situated at about 1 eV above the Fermi level, and push $5d$ and the upper π states toward the Fermi level. This is the reason why Ba_6C_{60} also becomes a semimetal.

VI. In short

I have presented our LDA calculations for a defect in Si, an initial stage of heteroepitaxy, and an alkaline-earth doped C_{60}. Of course, there remain several issues unclarified. But the LDA calculations provide us fair description of the phenomena in a variety of materials.

Acknowledgment

I wish to thank 0 . Sugino, M. Saito, B. D. Yu. and S. Saito for collaboration in a part of the work presented in this article. 1 also benefit from useful discussion with Y. Miyamoto.

References

1 P. Hohenberg and W. Kohn, Phys. Rev. **136**, B864 (1965); W. Kohn and L. J. Sham, Phys. Rev. **140**, A1133 (1965).
2. For a review, see *Theory of the Inhomogeneous Electron Gas* edited by S. Lundqvist and N. H. March (Plenum, N.Y. 1983).
3. M. S. Hybertsen and S. G. Louie, Pliys. Rev. Lett. 55, 1418 (1985); Phys. Rev. **B34**, 5390 (1986).
4. A. Oshiyama and M. Saito, J. Phys. Soc. Jpn. 56, 2104 (1987); M. Saito, A. Oshiyama and O. Sugino, Phys. Rev. B45, 13745 (1992).
5. O. Sugino and A. Oshiyama, Pliys. Rev. Lett. **68**, 1858 (1992).
6. D. R. Hitmann, M. Schlüter and C. Chiang, Pliys. Rev. Lett. 43, 1494 (1979); N. Troullier and J. L. Martins, Phys. Rev. B43, 1993 (1991).
7. D. M. Ceperley and B. J. Alder, Pliys. Rev. Lett,. 45, 566 (1980).
8. J. P. Perdew and A. Zunger, Pliys. Rev. **B23**, 5048 (1981).
9. In the calculations for fullerides presented in this talk, we use gaussian-orbital basis sets. For the comparison with the results from the plane-wave-basis sets, see ref.
10. O. Sugino and A. Oshiyama, *Proc. 16th Int. Conf. Defects in Semiconductors* (Trans Tech, Lehigh, 1991) p.469.
11. R. Car and M. Parrinello, Phys. Rcv. Lett,. 55, 2471 (1935).
12. L. Kleinman and D. M. Bylander, Phys. Rev. Lett. 48 1425 (1982).
13. G. D. Watkins, in *Lattice Defects* in *Semiconductors, 1974* Institute of Physics Conference Series No. 23, pl.
14. F. G. Anderson, F. Ham and G. Grossmann, *Proc. 16th Int. Conf. Defects in Semiconductors* (Trans Tech, Lehigh, 1991) p.475.
15. M. Sprenger et al., Physica **116B**, 224 (1953); Phys. Rev. **B35**, 1566 (1987).
16. R. S. Becker, T. Klitsner and J. S. Vickers, J. Microsc. (Oxford) **152**, 157 (1988).
17. R. D. Bringans, D. K. Biegelsen and L.-E. Swartz, Phys. Rev. **B44**, 3054 (1991), and references therein.
18. O. L. Alerhand, J. Wang, J. D. Joannopoulos, E. Kaxiras and R. S. Becker, Phys. Rev. **B44**, 6534 (1991).
19. R. M. Tromp, A. W. Denier van der Gon, and M. C. Reuter, Pliys. Rev. Lett. 68, 2313 (1992).
20. B. D. Yu and A. Oshiyama, Phys. Rev. Lett. 71, 585 (1993).
21. H. W. Kroto, J. R. Heath, S. C. O'Brien, R. F. Curl and R. E. Smalley, Nature 318, 162 (1985); E. Osawa, Kagaku (Kyoto) 25, 854 (1970); S. Iijima, J. Cryst. Growth 50, 675 (1980).
22. W. Kratschmer, L. D. Lamb, K. Fostiropoulos and D. R. Huffman, Nature 347, 354 (1990).
23. S. Saito and A. Oshiyama, Phys. Rev. Lett. 66, 2637 (1991).
24. S. G. Louie and E. L. Shirley, Braz. J. Phys. 24, 43 (1994).
25. A. Hebard et al., Nature 350, 600 (1991); M. J. Rosseinsky et al., Phys. Rev. Lett. 66, 2830 (1991); K. Holczer et al., Sciencc 252, 1154 (1991); K. Tanigaki et al., Nature 352, 222 (1991).
26. For a review, A. Oshiyama, S. Saito, N. Hamada, and Y. Miyamoto, J. Phys. Çhem. Solids, 53, 1457 (1992).
27. A. Oshiyama and S. Saito, Solid State Commun., 82, 41 (1992).
28. A. R. Kortan et al., Nature 355, 529 (1992); For the electronic structure, see S. Saito and A. Oshiyama, Solid State Commun. 83, 107 (1992).
29. A. R. Kortan et al., Nature 360, 566 (1992).
30. A. R.. Kortan et al., to be published.
31. S. Saito and A. Oshiyama, Phys. Rev. Lett. 71, 121 (1993).
32. S. C. Erwin and M. R. Pederson, Phys. Rev. Lett. 67, 1610 (1991).